0026-895X/11/8006-1147–1155$25.00
MOLECULAR PHARMACOLOGY
Copyright © 2011 The American Society for Pharmacology and Experimental Therapeutics
Mol Pharmacol 80:1147–1155, 2011

Vol. 80, No. 6
74138/3732172
Printed in U.S.A.

Dynamic and Ligand-Selective Interactions of Vitamin D Receptor with Retinoid X Receptor and Cofactors in Living Cells

Mihwa Choi, Sachiko Yamada, and Makoto Makishima

Division of Biochemistry, Department of Biomedical Sciences, Nihon University School of Medicine, Tokyo, Japan

Received June 13, 2011; accepted September 14, 2011

ABSTRACT

The vitamin D receptor (VDR) mediates vitamin D signaling in numerous physiological and pharmacological processes, including bone and calcium metabolism, cellular growth and differentiation, immunity, and cardiovascular function. Although transcriptional regulation by VDR has been investigated intensively, an understanding of ligand-selective dynamic VDR conformations remains elusive. Here, we examined ligand-dependent dynamic interactions of VDR with retinoid X receptor (RXR), steroid receptor coactivator 1 (SRC-1), and silencing mediator of retinoic acid and thyroid hormone receptor (SMRT) in cells using fluorescence resonance energy transfer (FRET) and chromatin immunoprecipitation (ChIP) assays. We compared the effects of 1α,25-dihydroxyvitamin D_3 [1,25$(OH)_2D_3$], lithocholic acid (LCA), and (25*R*)-25-adamantyl-1α,25-dihydroxy-2-methylene-22,23-didehydro-19,26,27-trinor-20-epivitamin D_3 (ADTT), a partial agonist/antagonist vitamin D derivative. In the absence of ligand, VDR homodimers were preferred to RXR heterodimers and were associated with SMRT. 1,25$(OH)_2D_3$ induced heterodimerization with RXR, dissociation of SMRT, and association of SRC-1. LCA and ADTT induced those effects to a lesser extent at concentrations that did not induce expression of the VDR target gene *CYP24A1* in human embryonic kidney (HEK) 293 cells. Unlike in HEK293 cells, ADTT increased CYP24A1 expression in HCT116 cells and increased the association of VDR and SMRT on the CYP24A1 promoter. The results indicate that ligand-selective conformation may lead to unique cofactor complex formation in a cell context-dependent manner. The combination of FRET and ChIP assays is a powerful tool useful in understanding ligand-selective dynamic VDR conformations and the development of selective VDR modulators.

Introduction

The vitamin D receptor (VDR; NR1I1), a member of the nuclear receptor superfamily, mediates the biological action of the active form of vitamin D, 1α,25-dihydroxyvitamin D_3 [1,25$(OH)_2D_3$], and regulates calcium and bone homeostasis, immunity, and cellular growth and differentiation (Haussler et al., 1998). Forty-eight human nuclear receptors have been identified, including endocrine receptors for steroid and thyroid hormones, metabolic sensors for fatty acids, bile acids, oxysterols and xenobiotics, and orphan receptors whose natural ligands are unknown (Makishima, 2005). Like other nuclear hormone receptors, VDR is activated in a ligand-dependent manner. On ligand binding, VDR undergoes a conformational change in the cofactor binding site and activation function 2 (AF2) surface, a structural rearrangement that results in a dynamic exchange of cofactor complexes (Makishima and Yamada, 2005). In the absence of ligand, corepressors bind to the AF2 surface, composed of portions of helix 3, loops 3 and 4; helices 4 and 5; and helix 11. Ligand binding alters the AF2 surface by repositioning helix 12, reducing the affinity for corepressors and increasing affinity for coactivator recruitment, a structural rearrangement that allows nuclear receptors to induce transcription of specific genes. Ligand-bound VDR not only mediates transactivation but also can mediate transrepression in some contexts (Fujiki et al., 2005). Dynamic and coordinated interaction of VDR with cofactor complexes is required for the efficient regulation of transcription. VDR binds preferentially to a vitamin D response element that consists of a two-hexanucleotide (AGGTCA or a related sequence) motif as a heterodimer with the retinoid X receptor (RXR; NR2B) (Haussler et al., 1998). Al-

This work was supported in part by the Ministry of Education, Culture, Sports, Science and Technology [Grant-in-Aid for Scientific Research on Priority Areas 18077005], the Japan Society for the Promotion of Science [Grant-in-Aid for JSPS Fellows 19-07197] (to M.C.); and the Naito Foundation.

Article, publication date, and citation information can be found at http://molpharm.aspetjournals.org.

doi:10.1124/mol.111.074138.

ABBREVIATIONS: VDR, vitamin D receptor; 1,25$(OH)_2D_3$, 1α,25-dihydroxyvitamin D_3; AF2, activation function 2; RXR, retinoid X receptor; FRET, fluorescence resonance energy transfer; GST, glutathione transferase; ADTT, (25*R*)-25-adamantyl-1α,25-dihydroxy-2-methylene-22,23-didehydro-19,26,27-trinor-20-epivitamin D_3; LCA, lithocholic acid; EYFP, enhanced yellow fluorescent protein; ID, interacting domain; SRC-1, steroid receptor coactivator 1; SMRT, silencing mediator of retinoic acid and thyroid hormone receptor; Tk, thymidine kinase; LUC, luciferase; HEK, human embryonic kidney; PCR, polymerase chain reaction; ChIP, chromatin immunoprecipitation.

though RXR acts as a receptor for 9-*cis* retinoic acid, the VDR-RXR heterodimer is not permissive to RXR ligand activation. VDR is highly expressed in target organs that mediate calcium homeostasis, such as the intestine, bone, kidney, and parathyroid glands. VDR response elements have been identified in regulatory regions of many target genes, including vitamin D 24-hydroxylase (CYP24A1), calbindin D9k, and transient receptor potential vanilloid type 6 (Choi and Makishima, 2009). Genes involved in xenobiotic metabolism, inflammation, and cell growth are also regulated by VDR activation (Nagpal et al., 2005).

An understanding of the physiological and pharmacological properties of $1,25(OH)_2D_3$ reveals that VDR is a promising drug target in the treatment of cancers, autoimmune diseases, infections, and cardiovascular diseases as well as bone and mineral disorders (Choi and Makishima, 2009). A number of vitamin D derivatives have been synthesized and evaluated for therapeutic application (Carlberg, 2003). Although they have been used successfully in the treatment of bone, mineral, and skin disorders, adverse effects (hypercalcemia in particular) limit their clinical application. Therefore, the development of VDR ligands that lack hypercalcemic action is required to realize the potential of VDR-targeted therapy. The molecular basis of function-selective or nonhypercalcemic VDR ligands can be tested with in vitro and in vivo assays, including VDR interaction, regulation of cofactor recruitment, pharmacokinetics, and cell type- or tissue-selective action (Choi and Makishima, 2009). With an improved understanding of the mechanisms of VDR signaling, the possibility of identifying VDR ligands with selective action is emerging.

Fluorescence resonance energy transfer (FRET), a method to monitor protein-protein interaction, has been successfully used in studies of nuclear receptor dimerization and cofactor interaction for the estrogen receptor, androgen receptor, retinoic acid receptor, and peroxisome proliferator-activated receptor in living cells (Llopis et al., 2000; Bai and Giguére, 2003; Feige et al., 2005; Schaufele et al., 2005). Ligand-selective interactions of VDR with RXR and cofactors have been investigated using techniques such as the mammalian two-hybrid assay and a glutathione transferase (GST) pull-down assay (Peräkylä et al., 2005; Ma et al., 2006; Inaba et al., 2007). In this study, we applied FRET in living cells to evaluate the interaction of VDR with RXRα and cofactors stimulated by $1,25(OH)_2D_3$, (25*R*)-25-adamantyl-1α,25-dihydroxy-2-methylene-22,23-didehydro-19,26,27-trinor-20-epivitamin D_3 (ADTT), and lithocholic acid (LCA). ADTT is a synthetic vitamin D derivative that shows partial agonist/antagonist activity (Nakabayashi et al., 2008). LCA is a secondary bile acid that acts as an additional physiological VDR agonist (Makishima et al., 2002). Our results show that $1,25(OH)_2D_3$, ADTT, and LCA induce distinct complexes of VDR with RXR and cofactor fragments and that these complexes are recruited to the CYP24A1 promoter in a cell type-specific manner. Our findings provide evidence for the dynamic regulation of ligand-selective VDR-cofactor complexes in vivo.

Materials and Methods

Chemical Compounds. $1,25(OH)_2D_3$ was purchased from Wako Pure Chemical Industries (Osaka, Japan), and LCA was from Nacalai Tesque, Inc. (Kyoto, Japan). ADTT was synthesized in our laboratory (Nakabayashi et al., 2008).

Plasmids. A fragment of human VDR (amino acids 2–427; GenBank accession no. NM_000376) was inserted into Clontech pAmCyan1-C1 and pEYFP-C1 (Takara Bio Inc., Otsu, Japan) to make pAmCyan-VDR and pEYFP-VDR, respectively. Fragments of RXRα (amino acids 2–462; GenBank accession no. NM_002957), nuclear receptor-interacting domain (ID) 1 to 3 (amino acids 595–771) and ID4 (amino acids 1345–1441) of steroid receptor coactivator 1 (SRC-1) (GenBank accession no. NM_003743), and ID1 (amino acids 2096–2182), ID2 (amino acids 2278–2514), and ID1 + ID2 (amino acids 2096–2514) of silencing mediator of retinoic acid and thyroid hormone receptor (SMRT) (GenBank accession no. NM_006312) were inserted into pEYFP-C1 to make pEYFP-RXR, pEYFP-SRC-1 (ID1–ID3), pEYFP-SRC-1 (ID4), pEYFP-SMRT (ID1), pEYFP-SMRT (ID2), and pEYFP-SMRT (ID1 + ID2), respectively. Fragments of SRC-1 (ID4), SMRT (ID1), SMRT (ID2), and SMRT (ID1 + ID2) were inserted into the pCMX-GAL4 vector to make pCMX-GAL4-SRC-1 (ID4), pCMX-GAL4-SMRT (ID1), pCMX-GAL4-SMRT (ID2), and pCMX-GAL4-SMRT (ID1 + ID2), respectively (Igarashi et al., 2007; Inaba et al., 2007). pCMX-VDR, pCMX-VP16-VDR, pCMX-GAL4-SRC-1 (ID1–ID3; amino acids 595–771), Sppx3-tk-LUC, and MH100(UAS)x4-tk-LUC were previously reported (Igarashi et al., 2007; Inaba et al., 2007). All plasmids were sequenced before use to verify DNA sequence fidelity.

Cell Culture and Transfection Assays. HEK293 cells, colon carcinoma HCT116 cells, immortalized keratinocyte HaCaT cells, and monkey kidney COS-7 cells were cultured in Dulbecco's modified Eagle's medium containing 10% fetal bovine serum, 100 units/ml penicillin, and 100 μg/ml streptomycin at 37°C in a humidified incubator containing 5% CO_2. Human osteosarcoma MG63 cells were maintained in minimum essential medium containing 10% fetal bovine serum.

For FRET, cells were seeded in six-well plates or glass-bottomed dishes and transfected with 1 μg of each fluorescent protein expression plasmid using FuGENE HD (Roche Applied Science, Indianapolis, IN) according to the manufacturer's instructions. For luciferase reporter assays, transfection in HEK293 cells was performed via calcium phosphate coprecipitation (Inaba et al., 2007). Transfection used 50 ng of a reporter plasmid (Sppx3-tk-LUC for VDR or MH100(UAS)x4-tk-LUC for GAL4), 15 ng of each expression plasmid, and 10 ng of pCMX-β-galactosidase for each well of 96-well plate (Igarashi et al., 2007; Inaba et al., 2007). Luciferase data were normalized to an internal β-galactosidase control.

GST Pull-Down Assay. GST fusion proteins were expressed in BL21 DE3 cells (Promega Corporation, Madison, WI) and purified using glutathione Sepharose 4B (GE Healthcare, Chalfont St. Giles, Buckinghamshire, UK). ^{35}S-labeled proteins were generated using a TNT Quick-Coupled Transcription/Translation System (Promega Corporation). GST pull-down assays were performed as reported previously (Inaba et al., 2007). GST proteins were incubated with reticulocyte lysate containing ^{35}S-labeled proteins and were treated with test compounds for 2 h at 4°C.

Immunoprecipitation and Immunoblotting. HEK293 cells were transfected with pCMX-FLAG-VDR in combination with pCMX-GAL4-SRC-1 (ID1–ID3) or pCMX-GAL4-SRC-1 (ID4) and were treated with ligand for 1 h. Cell lysates were subjected to immunoprecipitation with anti-FLAG antibody (Sigma-Aldrich, St. Louis, MO). Immunocomplexes were separated by SDS-polyacrylamide gel electrophoresis, transferred to a membrane, probed with anti-GAL4 antibody (Santa Cruz Biotechnology, Inc., Santa Cruz, CA), and visualized with enhanced chemiluminescence (GE Healthcare).

Reverse Transcription and Quantitative Real-Time PCR Analysis. Total RNAs from cells were prepared using an RNAgents Total RNA Isolation System (Promega, Madison, WI), and cDNAs were synthesized with an ImProm-II Reverse Transcription System (Promega). Quantitative real-time PCR was performed on an ABI PRISM 7000 Sequence Detection System (Applied Biosystems, Foster City, CA) with Power SYBR Green PCR Master Mix (Applied Biosystems) (Nishida et al., 2009). Primers were as follows: CYP24,

5′-GTT TGG GAG GAT GAT GGT CAC T-3′ and 5′-AGT GTG TCC CTG CCA GAC CTT-3′; cyclophilin A, 5′-GGA GAT GGC ACA GGA GGA A-3′ and 5′-GCC CGT AGT GCT TCA GTT T-3′. mRNA values were normalized to an amount of cyclophilin A mRNA.

FRET. FRET measurements were performed with a spectrofluorophotometer as described previously with minor modifications (Baneyx et al., 2001; Erickson et al., 2003). HEK293 cells were transfected with expression plasmids for AmCyan (excitation maximum, 453 nm; emission maximum, 486 nm) and EYFP (excitation maximum, 513 nm; emission maximum, 527 nm). Forty-eight hours after transfections, ligands were added. After treatment for 30 or 60 min, cells were washed in ice-cold phosphate-buffered saline, sonicated, and centrifuged. Fluorescence of supernatants was measured with an RF-1500 spectrofluorophotometer (Shimadzu Corporation, Kyoto, Japan). Fluorescent emission spectra were recorded with excited AmCyan at 450 nm. FRET was calculated as a ratio of the emission maximum of EYFP to that of AmCyan (526 ± 2 nm/488 ± 2 nm) as reported previously for FRET from europium to allophycocyanin (Makishima et al., 1999).

For FRET in living cells, COS-7 cells were transfected with expression plasmids for fluorescent fusion proteins and were cultured on a glass-bottomed dish. Forty-eight hours after transfection, ligands were added. Cells were washed with phosphate-buffered saline, replaced in phenol red-free Dulbecco's modified Eagle's medium, and observed with a TCS SP-5 fluorescence confocal microscope (Leica Microsystems, Wetzlar, Germany) with a Plan-Apochromat 63×/1.4 numerical aperture oil objective lens (Leica Microsystems). Excitation light intensities were calibrated using an objective with a laser power meter. Cell images were acquired in exciting AmCyan from 458 nm as described previously (Zwart et al., 2007). Emission spectra were detected with a photomultiplier tube. A pinhole was set to 1 Airy unit with a scanning frequency of 1000 Hz.

Chromatin Immunoprecipitation Assays. Chromatin immunoprecipitation (ChIP) assays were performed as described previously with minor modifications (Shang et al., 2000; Matsunawa et al., 2009). Cells were fixed with 1% formaldehyde for 10 min at room temperature. ChIP was performed with a ChIP Assay Kit (Millipore, Billerica, MA) and anti-VDR, anti-RXR, anti-SRC-1, anti-SMRT, or control IgG antibodies (Santa Cruz Biotechnology). For sequential ChIP, immune complexes were first eluted by incubation with 10 mM dithiothreitol at room temperature for 30 min (Shang et al., 2000). After dilution, eluted samples were incubated with a second antibody overnight at 4°C. After purification of DNA from the immunoprecipitated chromatin complexes, quantitative PCR was performed using Power SYBR Green PCR Master Mix (Applied Biosystems) with primers for CYP24A1 (5′-CAT CGC GAT TGT GCA AGC-3′ and 5′-CAA TGA GCA CGC AGA GG-3′).

Statistics. Values are shown as means ± 1 S.D. The unpaired two-group Student's *t* test was performed to assess significant differences.

Results

Induction of FRET between AmCyan-VDR and EYFP-RXR by VDR Ligands. To establish a FRET assay for the interaction of VDR, RXR and cofactors, we examined spectroscopic properties of four fluorescent chromophores: two variants of green fluorescent protein (enhanced cyan fluorescent protein and EYFP) and two coral fluorescent proteins (AmCyan and ZsYellow). The four fluorescent proteins were expressed individually or as a donor-acceptor pair (enhanced cyan fluorescent protein and EYFP, AmCyan and EYFP, or AmCyan and ZsYellow) in HEK293 cells, and the fluorescent spectra of the cell lysates were analyzed. Spectral analysis of the cell lysate showed acceptable parameters for the AmCyan and EYFP pair (data not shown). We examined ligand-induced transactivation of VDR fused to AmCyan or EYFP by a luciferase reporter assay. We transiently transfected HEK293 cells with an expression vector for AmCyan-VDR or EYFP-VDR (Fig. 1A) and a luciferase reporter containing a VDR-responsive direct repeat-3 element from the mouse osteopontin promoter (Igarashi et al., 2007) and measured $1,25(OH)_2D_3$-dependent luciferase activity. $1,25(OH)_2D_3$ (100 nM) effectively induced transactivation of wild-type VDR, AmCyan-VDR, and EYFP-VDR but not of control empty vector, AmCyan, or EYFP (Fig. 1B). These results show that ligand-dependent transactivation of AmCyan-VDR and EYFP-VDR is comparable with that of wild-type VDR.

Prüfer et al. has reported that GFP-VDR and RXRα-blue fluorescent proteins form heterodimers in the absence of ligand and that $1,25(OH)_2D_3$ treatment induces the formation of multiple nuclear foci of heterodimers (Prüfer et al., 2000). We have reported a ligand-independent interaction of VDR with RXR, which is enhanced by $1,25(OH)_2D_3$ using a mammalian two-hybrid assay (Inaba et al., 2007). We investigated the interaction of VDR with RXR using a FRET fluorophore pair of AmCyan-VDR and EYFP-RXR (Fig. 2A). Although exciting AmCyan at 450 nm results in emission at 488 nm unless energy is transferred to EYFP, FRET from AmCyan to EYFP yields the acceptor emission at 526 nm, resulting in an increased ratio of 526 nm/488 nm. First, we transfected HEK293 cells with AmCyan-VDR and EYFP-RXR expression plasmids and measured emission spectra in the cell lysates. Emission spectra at 450 nm excitation showed an intensity ratio (526 nm/488 nm) of 0.70 ± 0.08 (Table 1). An intensity ratio of a parent fluorophore pair of AmCyan and EYFP was 0.55 ± 0.10 ($p < 0.01$ versus AmCyan-VDR and EYFP-RXR pair) and that of an AmCyan-VDR and EYFP pair was 0.60 ± 0.10 ($p < 0.05$ versus

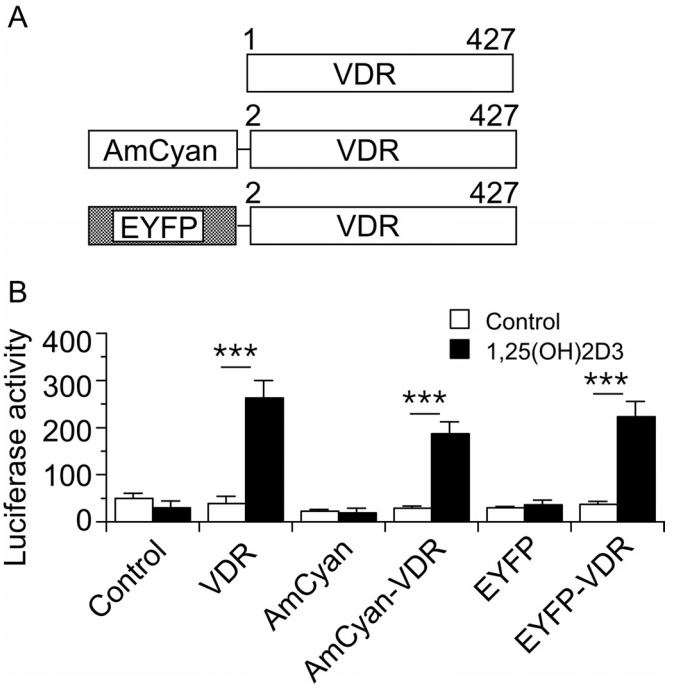

Fig. 1. Ligand-dependent transactivation of fluorescent-fused VDRs. A, AmCyan- and EYFP-fused VDRs. Numbers indicate amino acids. B, transactivation of AmCyan- and EYFP-fused VDRs. HEK293 cells were transfected with pCMX (control), pCMX-VDR, pAmCyan, pAmCyan-VDR, pEYFP, or pEYFP-VDR, and Sppx3-tk-LUC and treated with ethanol (control) or 100 nM $1,25(OH)_2D_3$. Values represent the means ± S.D. of triplicate assays. ***, $p < 0.001$.

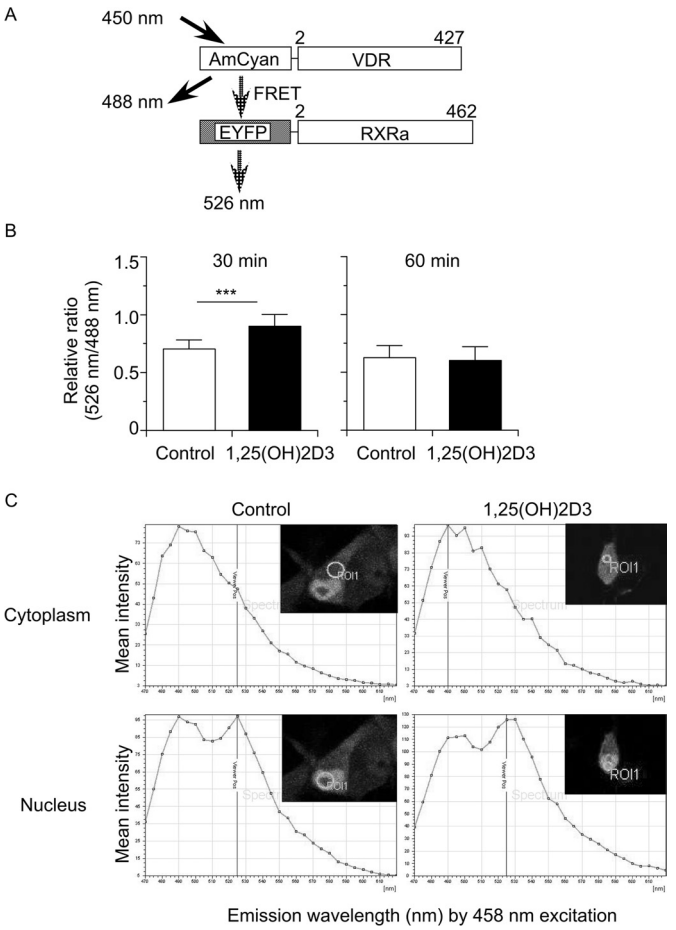

Fig. 2. $1,25(OH)_2D_3$ induces FRET between AmCyan-VDR and EYFP-RXR. A, principle of FRET. Exciting AmCyan at 450 nm results in emission at 488 nm, unless energy is transferred to EYFP. Energy transfer depends on the distance between AmCyan and EYFP. An increased EYFP emission (at 526 nm) at the expense of AmCyan emission can occur as the result of interaction between AmCyan-VDR and EYFP-RXR. Numbers indicate amino acids. B, $1,25(OH)_2D_3$ increases FRET between AmCyan-VDR and EYFP-RXR. HEK293 cells were transfected with pAmCyan-VDR and pEYFP-RXR and treated with ethanol (control) or 100 nM $1,25(OH)_2D_3$ for 30 or 60 min. Cell lysates were subjected to a spectrophotometer for a FRET assay. Values represent the means ± S.D. of septuplicate assays. ***, $p < 0.001$. C, induction of FRET between AmCyan-VDR and EYFP-RXR in the nucleus of COS-7 cells. COS-7 cells were transfected with pAmCyan-VDR and pEYFP-RXR and treated with ethanol (control) or 100 nM $1,25(OH)_2D_3$ for 30 min. Emission spectra were measured in the cytoplasm and nucleus with a fluorescence microscope. The experiments were repeated with similar results.

AmCyan-VDR and EYFP-RXR pair), indicating weak association of AmCyan-VDR and EYFP-RXR in the absence of ligand. When cells were treated with $1,25(OH)_2D_3$ (100 nM) for 30 min, an emission spectrum showed an increased intensity ratio of 0.90 ± 0.10 (Fig. 2B). The increased FRET in cells treated with $1,25(OH)_2D_3$ was no longer present at a 60-min time point.

Next, we expressed AmCyan-VDR and EYFP-RXR in COS-7 cells and examined FRET in living cells using confocal microscopy. Upon excitation at 458 nm, the cytoplasm showed an emission spectrum with a negligible FRET, and $1,25(OH)_2D_3$ treatment did not induce FRET (Fig. 2C), indicating that heterodimerization of VDR and RXR is negligible in the cytoplasm. In the nucleus, the emission spectrum showed two distinct peaks at 488 and 526 nm at nearly a 1:1 ratio, indicating that FRET occurs between AmCyan-VDR and EYFP-RXR in the

TABLE 1

The ratio of 526 nm/488 nm at 450 nm excitation

HEK293 cells were transfected with expression vectors for the indicated fluorescent proteins. Forty-eight hours after transfection, cell lysates were subjected to a spectrophotometer for FRET analysis. Values represent the means ± S.D. of triplicate or more assays.

Fluorophore pair	Ratio of 526 nm/488 nm
AmCyan only	0.48 ± 0.06
AmCyan + EYFP	0.55 ± 0.10
AmCyan-VDR only	0.52 ± 0.07
AmCyan-VDR + EYFP	0.60 ± 0.10
AmCyan-VDR + EYFP-VDR	0.94 ± 0.10
AmCyan-VDR + EYFP-RXR	0.70 ± 0.08
AmCyan-VDR + EYFP-SRC-1 (ID1–ID3)	0.90 ± 0.10
AmCyan-VDR + EYFP-SRC-1 (ID4)	0.76 ± 0.09
AmCyan-VDR + EYFP-SMRT (ID1)	0.88 ± 0.10
AmCyan-VDR + EYFP-SMRT (ID2)	1.41 ± 0.41
AmCyan-VDR + EYFP-SMRT (ID1 + ID2)	1.86 ± 0.19

absence of ligand. $1,25(OH)_2D_3$ treatment increased the intensity ratio (526 nm/488 nm) from 1.00 to 1.13 (Fig. 2C). Thus, $1,25(OH)_2D_3$ binding to VDR enhances heterodimerization of nuclear VDR and RXR.

VDR homodimerization has been reported (Cheskis and Freedman, 1994; Lemon and Freedman, 1996), but the existence of VDR homodimers in vivo is controversial. We examined VDR homodimerization by evaluating FRET between AmCyan-VDR and EYFP-VDR (Fig. 1A). In the absence of ligand, an emission spectrum in lysates of HEK293 cells expressing AmCyan-VDR and EYFP-VDR revealed an intensity ratio (526 nm/488 nm) of 0.94 ± 0.10, indicating a significant interaction compared with that of AmCyan-VDR and EYFP (0.60 ± 0.10; $p < 0.05$) (Table 1). $1,25(OH)_2D_3$ treatment for 30 min decreased FRET and this effect disappeared at 60 min (Fig. 3). Thus, $1,25(OH)_2D_3$ binding to VDR induces heterodimerization with RXR and inhibits homodimerization in cells.

ADTT is a synthetic vitamin D derivative that acts as a partial agonist/antagonist for VDR and LCA is a weak endogenous agonist (Makishima et al., 2002; Nakabayashi et al., 2008) (Fig. 4A). ADTT (10 μM) and LCA (10 μM) induced VDR transactivation (Fig. 4B). LCA (10 μM) but not ADTT (10 μM) increased a FRET signal between AmCyan-VDR and EYFP-RXR (Fig. 4C). The rank order of transactivation is the same as that of VDR-RXR heterodimerization: $1,25(OH)_2D_3$ (100 nM) > LCA (10 μM) > ADTT (10 μM).

Ligand-Dependent Interactions of VDR with Cofactors. Upon ligand binding, nuclear receptors undergo confor-

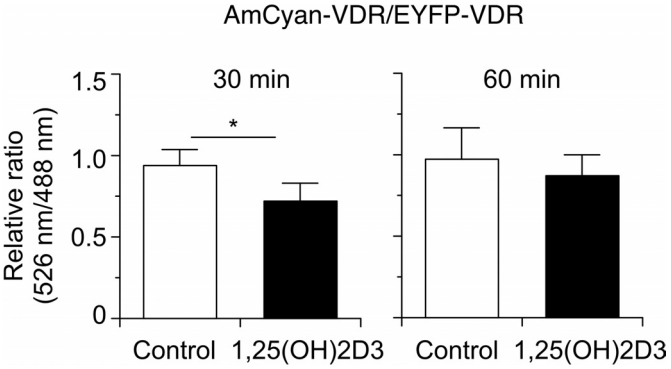

Fig. 3. $1,25(OH)_2D_3$ decreases VDR homodimerization. HEK293 cells were transfected with pAmCyan-VDR and pEYFP-VDR and treated with ethanol (control) or 100 nM $1,25(OH)_2D_3$ for 30 or 60 min. Cell lysates were subjected to a spectrophotometer for a FRET assay. Values represent the means ± S.D. of septuplicate assays. *, $p < 0.05$.

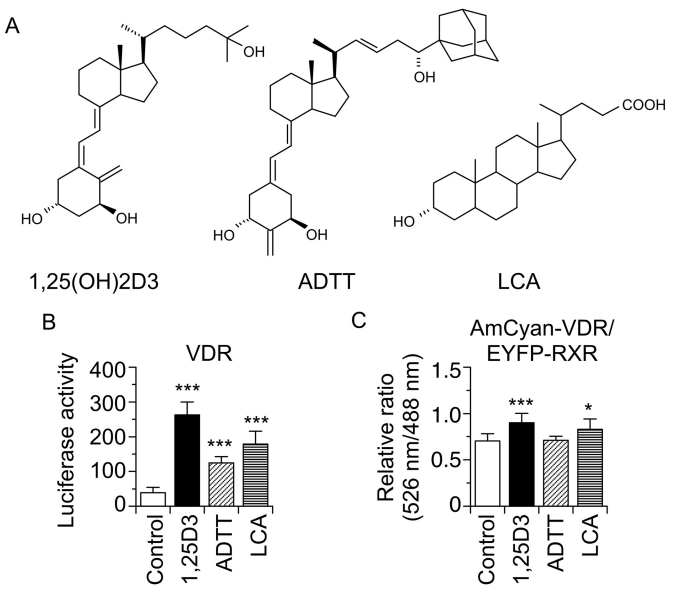

Fig. 4. Effect of $1,25(OH)_2D_3$, ADTT, and LCA on VDR-RXR heterodimerization. A, chemical structures of $1,25(OH)_2D_3$, ADTT, and LCA. B, transactivation of VDR. HEK293 cells were transfected with pCMX-VDR and Sppx3-tk-LUC and treated with ethanol (control), 100 nM $1,25(OH)_2D_3$, 10 μM ADTT, or 10 μM LCA. Values represent the means ± S.D. of triplicate assays. C, FRET between AmCyan-VDR and EYFP-RXR. HEK293 cells were transfected with pAmCyan-VDR and pEYFP-RXR and treated with ethanol (control), 100 nM $1,25(OH)_2D_3$, 10 μM ADTT, or 10 μM LCA for 30 min. Cell lysates were subjected to a spectrophotometer for a FRET assay. Values represent the means ± S.D. of quadruplicate assays. *, $p < 0.05$; ***, $p < 0.001$.

mational changes in the cofactor binding site and AF2 surface that result in the dissociation of corepressors and recruitment of coactivators (Rosenfeld et al., 2006). The p160 family proteins such as SRC-1 are well characterized coactivators that bind to the AF2 surface and transmit the allosteric signal of ligand binding to a chromatin remodeling system. We examined the effect of ligands on the interaction of VDR with SRC-1 using a mammalian two-hybrid assay and a FRET assay. We generated GAL4 fusions of SRC-1 (ID1–ID3) and SRC-1 (ID4) for the mammalian two-hybrid assay and their EYFP fusions for a FRET assay (Fig. 5A). EYFP-SRC-1 (ID1–ID3) contains three LXXLL motifs and has been shown to interact with VDR in a ligand-dependent manner (Adachi et al., 2004; Inaba et al., 2007). Results from a mammalian two-hybrid assay showed that $1,25(OH)_2D_3$, and to a lesser extent ADTT and LCA, effectively induced the interaction of VDR with the SRC-1 (ID1–ID3) fragment (Fig. 5B). $1,25(OH)_2D_3$, and ADTT increased FRET between AmCyan-VDR and EYFP-SRC-1 (ID1–ID3) at 30 min, and these associations disappeared at 60 min (Fig. 5C). LCA did not stabilize FRET between AmCyan-VDR and EYFP-SRC-1 (ID1–ID3). A SRC-1 domain including ID4 has been reported to be necessary for coactivation of the mineralocorticoid receptor (Li et al., 2005). In the mammalian two-hybrid assay, $1,25(OH)_2D_3$ but not ADTT or LCA induced the interaction of VDR with SRC-1 (ID4) (Fig. 5D). The FRET assay did not detect ligand-induced interaction between these proteins at 30 min (Fig. 5E). It is noteworthy that FRET was detected in cells treated with $1,25(OH)_2D_3$, ADTT and LCA at 60 min. Luciferase activity in a mammalian two-hybrid assay reflects the amount of luciferase protein in cultured cells and may represent an integrated value of the interaction over time. By contrast, the FRET assay detects the dynamic interaction of proteins at the selected 30- and 60-min time points. Discrepancies in the results between the mammalian two-hybrid assay and the FRET assay may be due to the two assays' differing ability to measure the strength of interaction over time. To further examine the interaction of VDR and SRC-1 (ID4), we performed GST pull-down and immunoprecipitation assays. $1,25(OH)_2D_3$ induced the interaction of GAL4-SRC-1 (ID1–ID3) and GAL4-SRC-1 (ID4) with GST-VDR but not with GST (Fig. 5F). GAL4 control proteins did not bind to GST-VDR in the presence or absence of $1,25(OH)_2D_3$ (data not shown). GAL4 fusion proteins of SRC-1 (ID1–ID3) and SRC-1 (ID4) bound to FLAG-VDR in cells, and $1,25(OH)_2D_3$ treatment enhanced these interactions (Fig. 5G). Thus, SRC-1 (ID4), like SRC-1 (ID1–ID3), binds to VDR in a ligand-dependent manner.

The corepressor SMRT has been reported to mediate transcriptional repression by unliganded VDR (Kim et al., 2009). SMRT has bipartite IDs (ID1 and ID2), each of which contains a LI/XXI/VI box (Fig. 6A). We generated GAL4 and EYFP fusions of SMRT (ID1), SMRT (ID2), and SMRT (ID1 + ID2). Treatment with $1,25(OH)_2D_3$ and ADTT but not LCA decreased the association of VP16-VDR and GAL4-SMRT (ID1) (Fig. 6B). An intensity ratio of a fluorophore pair of AmCyan-VDR and EYFP-SMRT (ID1) was 0.88 ± 0.10 ($p < 0.01$ versus AmCyan-VDR and EYFP pair), indicating interaction of these proteins (Table 1). $1,25(OH)_2D_3$ treatment did not change the FRET emission (Fig. 6C). ADTT, LCA, and to a lesser extent $1,25(OH)_2D_3$ decreased the interaction between VP16-VDR and GAL4-SMRT (ID2) (Fig. 6D). AmCyan-VDR and EYFP-SMRT (ID2) showed a strong FRET signal to 1.41 ± 0.41 ($p < 0.001$ versus AmCyan-VDR and EYFP pair) (Table 1), and $1,25(OH)_2D_3$, ADTT, and LCA decreased FRET (Fig. 6E). Treatment with $1,25(OH)_2D_3$, ADTT, and LCA decreased the association of VP16-VDR and GAL4-SMRT (ID1 + ID2) (Fig. 6F). Although $1,25(OH)_2D_3$, but not ADTT or LCA, decreased FRET between AmCyan-VDR and EYFP-SMRT (ID1 + ID2) at 30 min, FRET signals were decreased in cells treated with $1,25(OH)_2D_3$, ADTT and LCA for 60 min (Fig. 6G). Thus, SMRT IDs dissociate from VDR in a ligand-selective manner.

Ligand-Selective Recruitment of VDR, RXR, and Cofactors to an Endogenous Gene Promoter. We compared the effects of $1,25(OH)_2D_3$, ADTT, and LCA on the expression of an endogenous VDR target, CYP24A1, in kidney epithelium-derived HEK293 cells, osteoblast-derived MG63 cells, intestinal mucosa-derived HCT116 cells, and skin keratinocyte-derived HaCaT cells. As reported previously (Inaba et al., 2007), $1,25(OH)_2D_3$ effectively induced CYP24A1 expression in all of these cell lines (Fig. 7A). Although ADTT was not effective in HEK293 cells, it increased CYP24A1 expression in HCT116 cells, HaCaT cells, and, to a lesser extent, MG63 cells. The effect of ADTT (10 μM) was weaker than that of $1,25(OH)_2D_3$ (100 nM), indicating that ADTT is a partial agonist, consistent with VDR transactivation data (Fig. 4B) and a crystal structure of VDR and ADTT (Nakabayashi et al., 2008). LCA (10 μM) slightly increased CYP24A1 expression in HaCaT cells, but not in HEK293 cells, MG63 cells, or HaCaT cells (Fig. 7A), although it induced VDR transactivation in a luciferase reporter assay (Fig. 4B).

Next, we examined the recruitment of VDR, RXR, SRC-1, and SMRT to the CYP24A1 promoter using a ChIP assay in

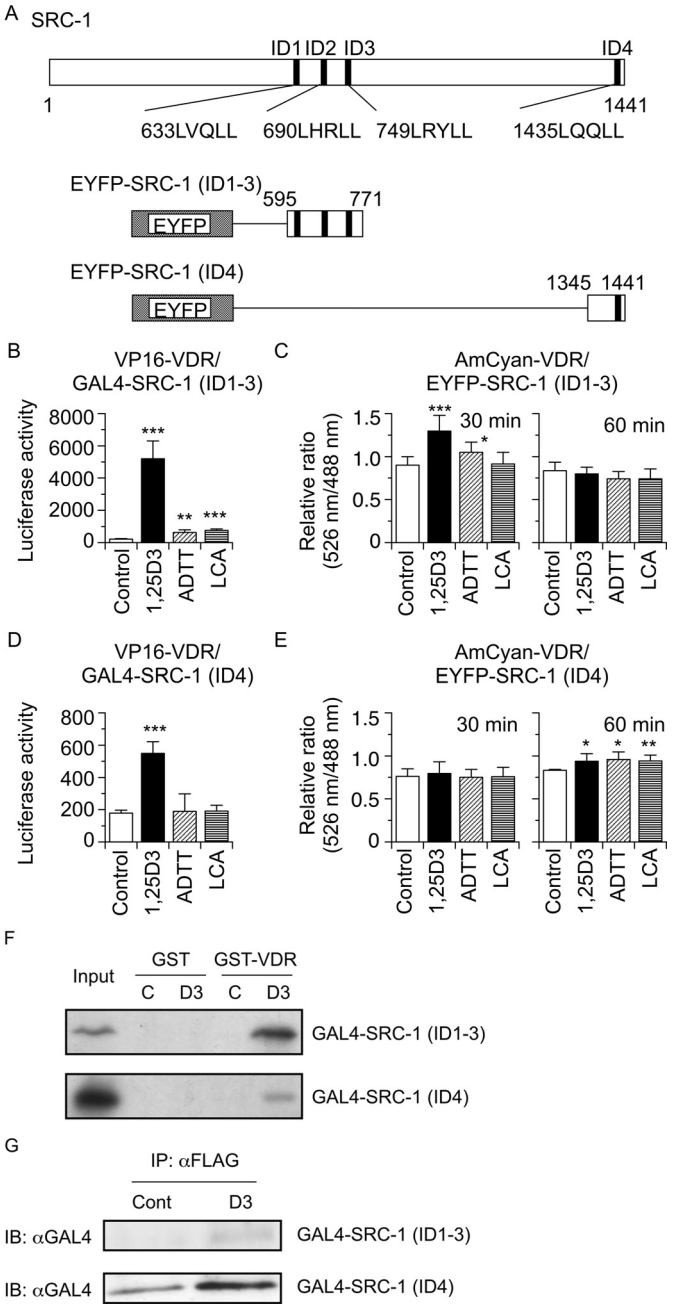

Fig. 5. Effect of $1,25(OH)_2D_3$, ADTT, and LCA on the VDR-SRC-1 interaction. A, EYFP-SRC-1 fusion proteins. Numbers indicate amino acids. B, a mammalian two-hybrid assay for VDR and SRC-1 (ID1–ID3) interaction. C, FRET between AmCyan-VDR and EYFP-SRC-1 (ID1–ID3). D, a mammalian two-hybrid assay for VDR and SRC-1 (ID4) interaction. E, FRET between AmCyan-VDR and EYFP-SRC-1 (ID4). For mammalian two-hybrid assays (B and D), HEK293 cells were transfected with pCMX-VP16-VDR; pCMX-GAL4-SRC-1 (ID1–ID3) or pCMX-GAL4-SRC-1 (ID4); and MH100(UAS)x4-tk-LUC and treated with ethanol (control), 100 nM $1,25(OH)_2D_3$, 10 μM ADTT, or 10 μM LCA. For FRET assays (C and E), HEK293 cells were transfected with pAmCyan-VDR and pEYFP-SRC-1 (ID1–ID3) or pEYFP-SRC-1 (ID4) and treated with ethanol (control), 100 nM $1,25(OH)_2D_3$, 10 μM ADTT, or 10 μM LCA for 30 and 60 min. Cell lysates were subjected to a spectrophotometer for a FRET assay. Values represent the means ± S.D. of triplicate assays. *, $p < 0.05$; *, $p < 0.01$; ***, $p < 0.001$. F, GST pull-down assays were performed to evaluate interactions between VDR and SRC-1 fragments. Control GST or GST-VDR proteins were incubated with ^{35}S-labeled GAL4-SRC-1 (ID1–ID3) or GAL4-SRC-1 (ID4) in the presence of ethanol (C) or 100 nM $1,25(OH)_2D_3$ (D3). G, in vivo interaction of VDR with SRC-1 fragments. HEK293 cells were transfected with pCMX-FLAG-VDR in combination with pCMX-GAL4-SRC-1 (ID1–ID3) or pCMX-GAL4-SRC-1 (ID4) and treated with ethanol (Cont) or 100 nM $1,25(OH)_2D_3$ (D3) for 1 h. Protein complexes in cell lysates were immunoprecipitated with anti-FLAG antibody and then immunoblotted with anti-GAL4 antibody. IP, immunoprecipitation; IB, immunoblotting.

HEK293 cells and HCT116 cells, because ADTT and LCA had no effect in HEK293 cells but ADTT exhibited agonist activity in HCT116 cells (Fig. 7A). Treatment with $1,25(OH)_2D_3$ for 30 and 60 min increased the occupancy of VDR, RXR, and SRC-1 on the CYP24A1 promoter in HEK293 cells (Fig. 7B). The $1,25(OH)_2D_3$-dependent recruitment of these proteins diminished at 120 min, consistent with the cyclic recruitment of VDR-RXR and coactivators that has been reported previously (Kim et al., 2005; Väisänen et al., 2005). SMRT associated with the CYP24A1 promoter region in the absence of ligand and $1,25(OH)_2D_3$ treatment decreased SMRT association (Fig. 7B). In contrast, ADTT treatment resulted in decreased recruitment of VDR to the CYP24A1 promoter (Fig. 7C). ADTT decreased SMRT association without increasing recruitment of RXR or SRC-1. LCA increased association of VDR and decreased that of SMRT. Thus, ADTT and LCA induce the recruitment of receptors and cofactors differently from $1,25(OH)_2D_3$. Similar to results in HEK293 cells, $1,25(OH)_2D_3$ increased the association of VDR, RXR, and SRC-1 and decreased that of SMRT on the CYP24A1 promoter in HCT116 cells (Fig. 7D). Although LCA induced dissociation of SMRT, it did not effectively recruit VDR, RXR, and SRC-1. It is noteworthy that ADTT increased the association of RXR and SMRT but not of VDR and SRC-1 in HCT116 cells. The interaction of SMRT to the CYP24A1 promoter was further examined with sequential ChIP analysis. Nuclear lysates of HCT116 cells were immunoprecipitated with anti-VDR antibody and re-ChIP was performed with anti-SMRT antibody. ADTT increased formation of the VDR- and SMRT-containing complex on the CYP24A1 promoter in HCT116 cells, whereas $1,25(OH)_2D_3$ did not (Fig. 7E). These findings suggest that ADTT and LCA are cell type-specific VDR modulators and that they exhibit selective recruitment of receptors and cofactors in a context-dependent manner.

Discussion

In this study, we observed ligand-selective dynamic interactions of VDR with RXR, SRC-1, and SMRT using FRET and ChIP assays. We used the AmCyan and EYFP fluorophore pair for FRET assays in living cells and cell lysates. In the absence of ligand, VDR preferentially formed homodimers and associated with SMRT (Table 1). $1,25(OH)_2D_3$ treatment induced VDR-RXR heterodimerization rather than VDR homodimerization (Fig. 2 and 3), consistent with previous reports (Cheskis and Freedman, 1994; Lemon and Freedman, 1996). FRET assays showed VDR-cofactor interactions, dissociation of SMRT, and recruitment of SRC-1, similar to the results of mammalian two-hybrid and ChIP assays (Fig. 5, 6, and 7). $1,25(OH)_2D_3$-dependent dissociation of SMRT (ID1) was observed in a mammalian two-hybrid assay but not in a FRET assay (Fig. 6). $1,25(OH)_2D_3$ decreased the FRET signal between VDR and SMRT (ID2) and induced a weak dissociation of SMRT (ID2) in the mammalian two-hybrid assay. VDR and RXR have been reported to interact with ID1 and ID2 of SMRT, respectively (Hu et al., 2001; Kim et al., 2009). Our results suggest that $1,25(OH)_2D_3$ binding first induces dissociation of ID2 from RXR

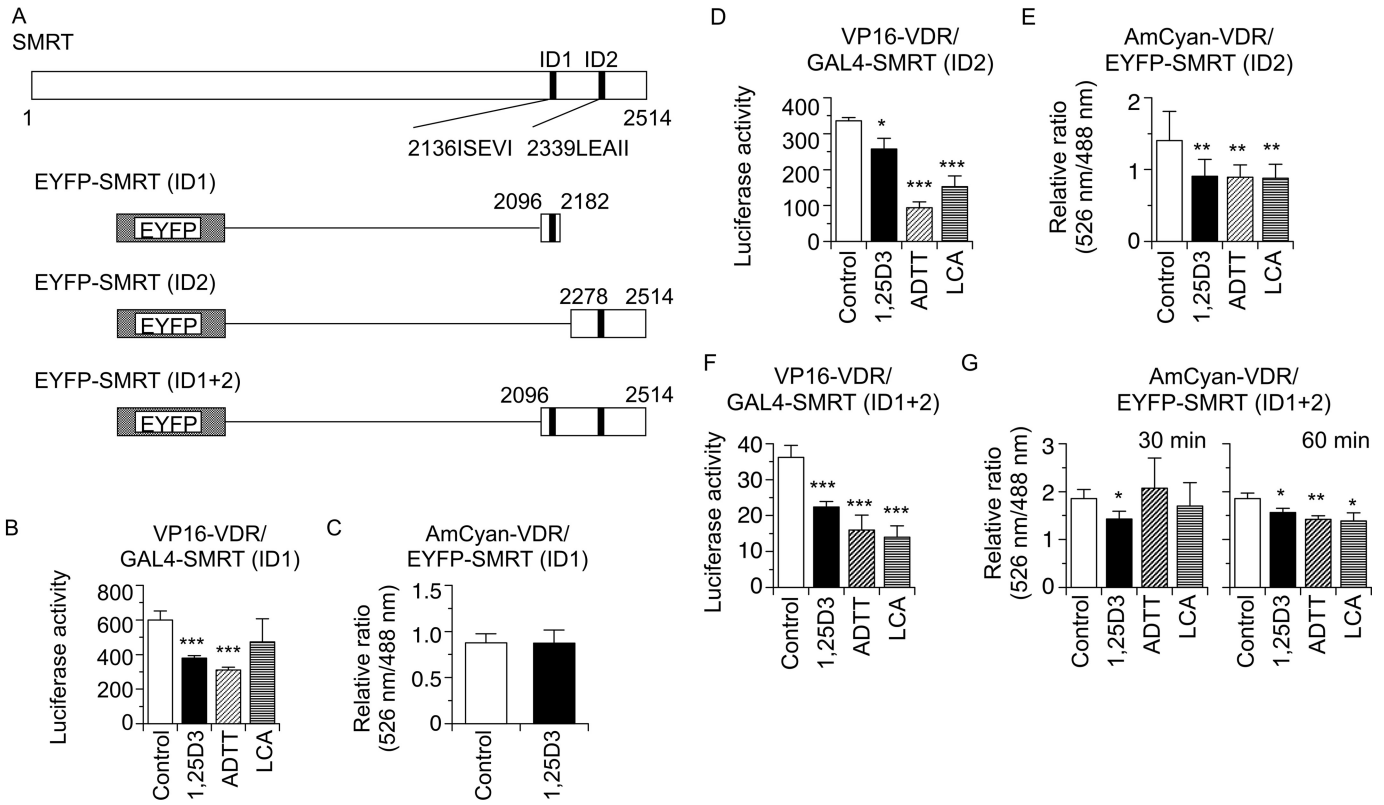

Fig. 6. Effect of $1,25(OH)_2D_3$, ADTT, and LCA on VDR-SMRT interaction. A, EYFP-SMRT fusion proteins. Numbers indicate amino acids. B, a mammalian two-hybrid assay for VDR and SMRT (ID1) interaction. C, FRET between AmCyan-VDR and EYFP-SMRT (ID1). D, a mammalian two-hybrid assay for VDR and SMRT (ID2) interaction. E, FRET between AmCyan-VDR and EYFP-SMRT (ID2). F, a mammalian two-hybrid assay for VDR and SMRT (ID1 + ID2) interaction. G, FRET between AmCyan-VDR and EYFP-SMRT (ID1 + ID2). For mammalian two-hybrid assays (B, D, and F), HEK293 cells were transfected with pCMX-VP16-VDR, pCMX-GAL4-SMRT (ID1), pCMX-GAL4-SMRT (ID2), or pCMX-GAL4-SMRT (ID1 + ID2), and MH100(UAS)x4-tk-LUC, and treated with ethanol (control), 100 nM $1,25(OH)_2D_3$, 10 μM ADTT, or 10 μM LCA. For FRET assays (C, E, and G), HEK293 cells were transfected with pAmCyan-VDR and pEYFP-SMRT (ID1), pEYFP-SMRT (ID2), or pEYFP-SMRT (ID1 + ID2) and treated with ethanol (control), 100 nM $1,25(OH)_2D_3$, 10 μM ADTT, or 10 μM LCA for 30 min (C, E, and G) and 60 min (G). Cell lysates were subjected to a spectrophotometer for a FRET assay. Values represent the means ± S.D. of triplicate assays (B–D, F, and G) or septuplicate assays (E). *, $p < 0.05$; *, $p < 0.01$; ***, $p < 0.001$.

in the VDR-RXR heterodimer and subsequently release of ID1 from VDR. The interaction of ID2 and RXR may play a principal role in the binding of the VDR-RXR heterodimer and SMRT in cells. Ligand-dependent dissociation of SMRT (ID1 + ID2) from VDR was different from those of SMRT (ID1) and SMRT (ID2) (Fig. 6), suggesting combined effects of ID1 and ID2 domains of SMRT on interaction with VDR-RXR heterodimer. Consistent with previous reports (Tagami et al., 1998; Pathrose et al., 2002; Adachi et al., 2004; Inaba et al., 2007), $1,25(OH)_2D_3$ was shown to induce association of VDR and SRC-1 (ID1–ID3) in mammalian two-hybrid and FRET assays (Fig. 5). In addition, $1,25(OH)_2D_3$ induced interaction between VDR and SRC-1 (ID4). SRC-1 (ID4) is necessary for coactivation of the mineralocorticoid receptor (Li et al., 2005). We found that VDR bound directly to SRC-1 (ID4) in a ligand-dependent manner (Fig. 5). Because a FRET assay showed $1,25(OH)_2D_3$-induced association of VDR and SRC-1 (ID4) at 60 min and not at 30 min (Fig. 5), this domain may play an accessory role in VDR-RXR coactivation. Thus, FRET assays are useful in the detection of time-dependent protein-protein interactions. The role of ID4 fragment in functional interaction between SRC-1 and VDR is under investigation.

LCA is a secondary bile acid that acts as a weak VDR agonist and interacts with the VDR ligand-binding pocket in a mode distinct from that of $1,25(OH)_2D_3$ (Makishima et al., 2002; Adachi et al., 2004). ADTT is a synthetic vitamin D derivative that acts as a VDR partial agonist/antagonist (Nakabayashi et al., 2008). LCA (10 μM) increased FRET between VDR and RXR but not between VDR and SRC-1 (ID1–ID3), whereas ADTT (10 μM) induced FRET between VDR and SRC-1 (ID1–ID3) but not between VDR and RXR (Figs. 4 and 5). ADTT and LCA at 10 μM were less effective than $1,25(OH)_2D_3$ (100 nM) in VDR transactivation in a luciferase reporter assay (Fig. 4) and did not induce endogenous CYP24A1 mRNA expression in HEK293 cells (Fig. 7). Neither ADTT nor LCA increased occupancy of RXR and SRC-1 on the CYP24A1 promoter (Fig. 7). Both heterodimerization with RXR and formation of an active conformation with coactivators are necessary for ligand-dependent VDR transactivation (Prüfer et al., 2000; Pathrose et al., 2002). These findings suggest that the conformation induced by ADTT and LCA is not sufficient to recruit a stable complex of VDR, RXR, and cofactors to a target gene needed to induce effective transcription. ADTT but not LCA induced dissociation of SMRT (ID1), and both ligands decreased association of VDR with SMRT (ID2) and SMRT (ID1 + ID2) (Fig. 6). VDR antagonists induce dissociation of corepressors as well as agonists (Inaba et al., 2007). Corepressor dissociation is suggested to reflect a ligand-dependent conformational change, and additional factors

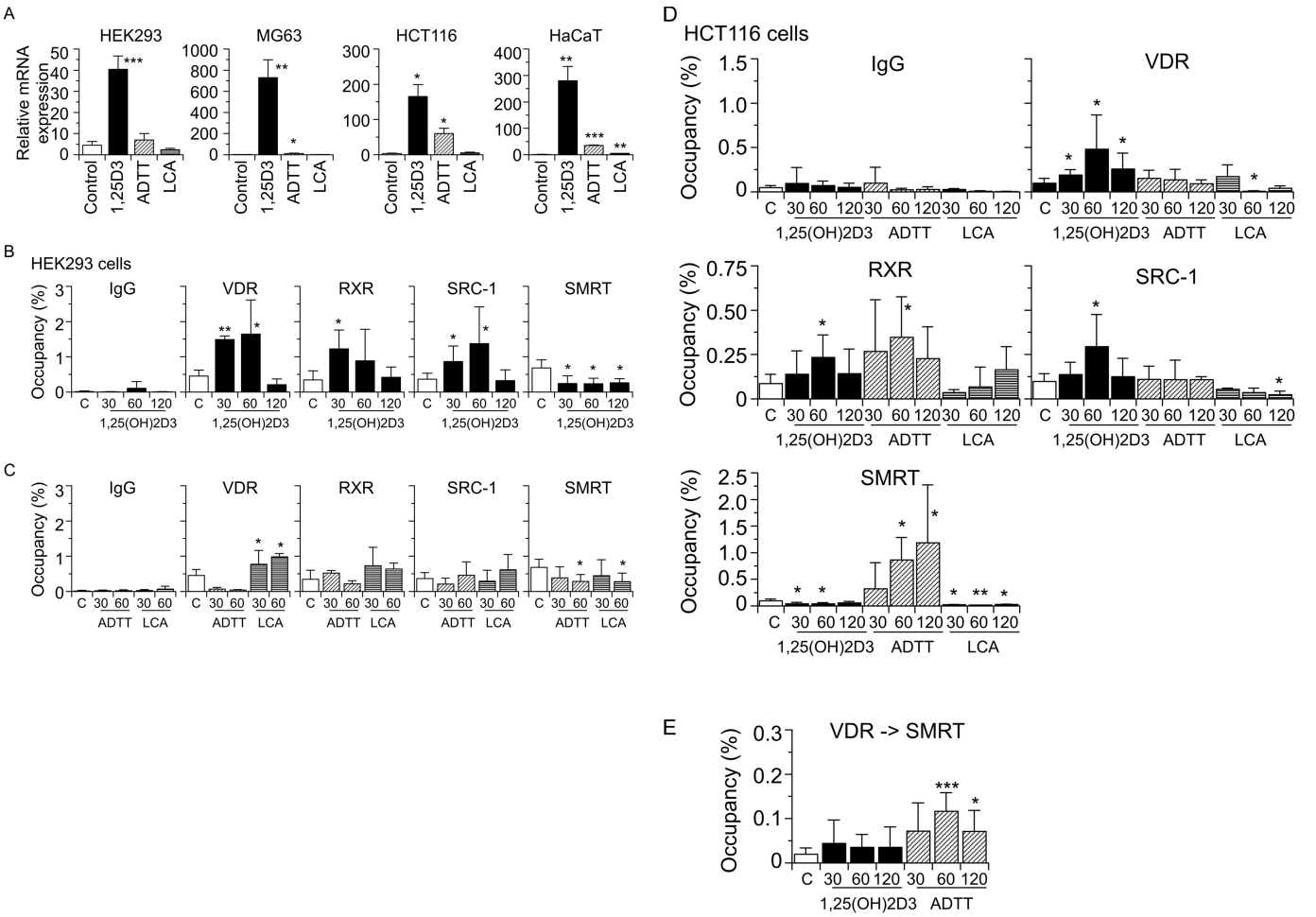

Fig. 7. Association of VDR, RXR, SRC-1, and SMRT on the CYP24A1 promoter in cells treated with $1,25(OH)_2D_3$, ADTT and LCA. A, expression of the *CYP24A1* gene in HEK293 cells, MG63 cells, HCT116 cells, and HaCaT cells. Cells were treated with ethanol (control), 100 nM $1,25(OH)_2D_3$ (1,25D3), 10 μM ADTT, or 10 μM LCA for 16 h. CYP24A1 mRNA levels were evaluated by quantitative real-time PCR. Values represent the means ± S.D. of triplicate assays. B and C, occupancy of VDR, RXR, SRC-1, and SMRT on the CYP24A1 promoter in HEK293 cells treated with $1,25(OH)_2D_3$ (B), ADTT, or LCA (C). HEK293 cells were treated with ethanol (C), 100 nM $1,25(OH)_2D_3$, 10 μM ADTT, or 10 μM LCA for 30, 60 or 120 min. Occupancy of the indicated proteins on the CYP24A1 promoter were examined with ChIP assays using control IgG, anti-VDR, anti-RXR, anti-SRC-1, or anti-SMRT antibodies. Occupancy (percentage) is relative to the input values. D, occupancy of VDR, RXR, SRC-1, and SMRT on the CYP24A1 promoter in HCT116 cells treated with $1,25(OH)_2D_3$, ADTT, or LCA. HCT116 cells were treated with ethanol (C), 100 nM $1,25(OH)_2D_3$, 10 μM ADTT, or 10 μM LCA for 30, 60 or 120 min, and ChIP assays were performed as in B and C. E, sequential ChIP with VDR and SMRT in HCT116 cells. ChIP samples with anti-VDR antibody as in D were next subjected with ChIP with anti-SMRT antibody. Values represent the means ± S.D. of triplicate assays. *, $p < 0.05$; *, $p < 0.01$; ***, $p < 0.001$.

such as stable complex with RXR and coactivators may be required for efficient transactivation.

Like AD47, another partial agonist/antagonist having an adamantane ring side chain (Inaba et al., 2007), ADTT induced endogenous CYP24A1 expression in HCT116 cells but not HEK293 cells (Fig. 7). ADTT, like $1,25(OH)_2D_3$ and LCA, decreased SMRT association on the CYP24A1 promoter in HEK293 cells, consistent with the results in mammalian two-hybrid and FRET assays. Unexpectedly, ADTT increased association of RXR and SMRT but not of VDR and SRC-1 on the CYP24A1 promoter in HCT116 cells. Although different occupancies of VDR and RXR on a CYP24A1 promoter region were reported (Matilainen et al., 2010), the mechanism of discrepancy in the recruitment of VDR and RXR remains unclear. ADTT may induce a complex of VDR-RXR heterodimer and cofactors that decreases the efficiency of ChIP with anti-VDR antibody. In a sequential ChIP assay, ADTT, but not $1,25(OH)_2D_3$, induced a complex of VDR and SMRT on the promoter. These findings suggest that ADTT induces a cofactor complex in a cell context-dependent manner. ADTT and $1,25(OH)_2D_3$ may induce distinct VDR conformations, resulting in the selective recruitment of cofactors. The subset of involved cofactors may be dependent on cell type-specific expression of cofactor proteins and other cellular environments. $1,25(OH)_2D_3$ recruits SMRT to the CYP24A1 promoter, and the corepressor is involved in negative transcriptional regulation (Sánchez-Martínez et al., 2008). We did not observe corecruitment of SRC-1 and SMRT to the CYP24A1 promoter in HCT116 cells. Ligand-dependent corepressor recruitment may be in a different phase from that of coactivators through a cyclic cell-selective pattern. Whereas $1,25(OH)_2D_3$ and LCA repress expression of the human cholesterol 7α-hydroxylase gene by recruiting SMRT to the VDR-RXR heterodimer (Han et al., 2010), SMRT has been reported to be involved in coactivation of estrogen receptor-α with SRC-3 on the progesterone receptor gene promoter (Karmakar et al., 2010). Further studies are needed to

elucidate the mechanism of agonist-dependent recruitment of SMRT and its functional relevance.

More than 2000 vitamin D derivatives have been synthesized and evaluated for potential therapeutic application (Carlberg, 2003). Although they have been used successfully in the treatment of bone, mineral and skin disorders, adverse effects, particularly hypercalcemia, limit the clinical application of vitamin D and its synthetic derivatives in the management of other diseases, such as cancer, autoimmunity, infection, and cardiovascular disease (Choi and Makishima, 2009). VDR interaction and cofactor recruitment as well as pharmacokinetics are key factors in designing VDR ligands with selective activity. In this study, we provided evidence for ligand-selective VDR conformations and cofactor recruitment using FRET and ChIP assays. These techniques will be useful in the further development of selective VDR modulators.

Acknowledgments

We thank Dr. Atsuko Iwane of the Graduate School of Frontier Biosciences, Osaka University, Osaka, Japan; Dr. Hiroki Nagase and Dr. Makoto Kimura of Nihon University Advanced Research Institute for the Science and Humanities, Tokyo, Japan; Dr. Kazumichi Kuroda and Toshikatsu Shibata of the Division of Microbiology, Department of Pathology and Microbiology, Nihon University School of Medicine; Sergej Popov, Daisuke Akagi, and other members of the Makishima laboratory for technical assistance and helpful comments; and Dr. Andrew I. Shulman for editorial assistance.

Authorship Contributions

Participated in research design: Choi, Yamada, and Makishima.
Conducted experiments: Choi.
Contributed new reagents or analytic tools: Choi and Yamada.
Performed data analysis: Choi, Yamada, and Makishima.
Wrote or contributed to the writing of the manuscript: Choi, Yamada, and Makishima.

References

Adachi R, Shulman AI, Yamamoto K, Shimomura I, Yamada S, Mangelsdorf DJ, and Makishima M (2004) Structural determinants for vitamin D receptor response to endocrine and xenobiotic signals. *Mol Endocrinol* **18:**43–52.
Bai Y and Giguére V (2003) Isoform-selective interactions between estrogen receptors and steroid receptor coactivators promoted by estradiol and ErbB-2 signaling in living cells. *Mol Endocrinol* **17:**589–599.
Baneyx G, Baugh L, and Vogel V (2001) Coexisting conformations of fibronectin in cell culture imaged using fluorescence resonance energy transfer. *Proc Natl Acad Sci USA* **98:**14464–14468.
Carlberg C (2003) Molecular basis of the selective activity of vitamin D analogues. *J Cell Biochem* **88:**274–281.
Cheskis B and Freedman LP (1994) Ligand modulates the conversion of DNA-bound vitamin D_3 receptor (VDR) homodimers into VDR-retinoid X receptor heterodimers. *Mol Cell Biol* **14:**3329–3338.
Choi M and Makishima M (2009) Therapeutic applications for novel non-hypercalcemic vitamin D receptor ligands. *Expert Opin Ther Pat* **19:**593–606.
Erickson MG, Moon DL, and Yue DT (2003) DsRed as a potential FRET partner with CFP and GFP. *Biophys J* **85:**599–611.
Feige JN, Gelman L, Tudor C, Engelborghs Y, Wahli W, and Desvergne B (2005) Fluorescence imaging reveals the nuclear behavior of peroxisome proliferator-activated receptor/retinoid X receptor heterodimers in the absence and presence of ligand. *J Biol Chem* **280:**17880–17890.
Fujiki R, Kim MS, Sasaki Y, Yoshimura K, Kitagawa H, and Kato S (2005) Ligand-induced transrepression by VDR through association of WSTF with acetylated histones. *EMBO J* **24:**3881–3894.
Han S, Li T, Ellis E, Strom S, and Chiang JY (2010) A novel bile acid-activated vitamin D receptor signaling in human hepatocytes. *Mol Endocrinol* **24:**1151–1164.
Haussler MR, Whitfield GK, Haussler CA, Hsieh JC, Thompson PD, Selznick SH, Dominguez CE, and Jurutka PW (1998) The nuclear vitamin D receptor: biological and molecular regulatory properties revealed. *J Bone Miner Res* **13:**325–349.
Hu X, Li Y, and Lazar MA (2001) Determinants of CoRNR-dependent repression complex assembly on nuclear hormone receptors. *Mol Cell Biol* **21:**1747–1758.
Igarashi M, Yoshimoto N, Yamamoto K, Shimizu M, Ishizawa M, Makishima M, DeLuca HF, and Yamada S (2007) Identification of a highly potent vitamin D receptor antagonist: (25S)-26-adamantyl-25-hydroxy-2-methylene-22,23-didehydro-19,27-dinor-20-epi-vitamin D_3 (ADMI3). *Arch Biochem Biophys* **460:**240–253.
Inaba Y, Yamamoto K, Yoshimoto N, Matsunawa M, Uno S, Yamada S, and Makishima M (2007) Vitamin D_3 derivatives with adamantane or lactone ring side chains are cell type-selective vitamin D receptor modulators. *Mol Pharmacol* **71:**1298–1311.
Karmakar S, Gao T, Pace MC, Oesterreich S, and Smith CL (2010) Cooperative activation of cyclin D1 and progesterone receptor gene expression by the SRC-3 coactivator and SMRT corepressor. *Mol Endocrinol* **24:**1187–1202.
Kim JY, Son YL, and Lee YC (2009) Involvement of SMRT corepressor in transcriptional repression by the vitamin D receptor. *Mol Endocrinol* **23:**251–264.
Kim S, Shevde NK, and Pike JW (2005) 1,25-Dihydroxyvitamin D_3 stimulates cyclic vitamin D receptor/retinoid X receptor DNA-binding, co-activator recruitment, and histone acetylation in intact osteoblasts. *J Bone Miner Res* **20:**305–317.
Lemon BD and Freedman LP (1996) Selective effects of ligands on vitamin D_3 receptor- and retinoid X receptor-mediated gene activation in vivo. *Mol Cell Biol* **16:**1006–1016.
Li Y, Suino K, Daugherty J, and Xu HE (2005) Structural and biochemical mechanisms for the specificity of hormone binding and coactivator assembly by mineralocorticoid receptor. *Mol Cell* **19:**367–380.
Llopis J, Westin S, Ricote M, Wang Z, Cho CY, Kurokawa R, Mullen TM, Rose DW, Rosenfeld MG, Tsien RY, et al. (2000) Ligand-dependent interactions of coactivators steroid receptor coactivator-1 and peroxisome proliferator-activated receptor binding protein with nuclear hormone receptors can be imaged in live cells and are required for transcription. *Proc Natl Acad Sci USA* **97:**4363–4368.
Ma Y, Khalifa B, Yee YK, Lu J, Memezawa A, Savkur RS, Yamamoto Y, Chintalacharuvu SR, Yamaoka K, Stayrook KR, et al. (2006) Identification and characterization of noncalcemic, tissue-selective, nonsecosteroidal vitamin D receptor modulators. *J Clin Invest* **116:**892–904.
Makishima M (2005) Nuclear receptors as targets for drug development: regulation of cholesterol and bile acid metabolism by nuclear receptors. *J Pharmacol Sci* **97:**177–183.
Makishima M, Lu TT, Xie W, Whitfield GK, Domoto H, Evans RM, Haussler MR, and Mangelsdorf DJ (2002) Vitamin D receptor as an intestinal bile acid sensor. *Science* **296:**1313–1316.
Makishima M, Okamoto AY, Repa JJ, Tu H, Learned RM, Luk A, Hull MV, Lustig KD, Mangelsdorf DJ, and Shan B (1999) Identification of a nuclear receptor for bile acids. *Science* **284:**1362–1365.
Makishima M and Yamada S (2005) Targeting the vitamin D receptor: advances in drug discovery. *Expert Opin Ther Pat* **15:**1133–1145.
Matilainen JM, Malinen M, Turunen MM, Carlberg C, and Väisänen S (2010) The number of vitamin D receptor binding sites defines the different vitamin D responsiveness of the CYP24 gene in malignant and normal mammary cells. *J Biol Chem* **285:**24174–24183.
Matsunawa M, Amano Y, Endo K, Uno S, Sakaki T, Yamada S, and Makishima M (2009) The aryl hydrocarbon receptor activator benzo[*a*]pyrene enhances vitamin D_3 catabolism in macrophages. *Toxicol Sci* **109:**50–58.
Nagpal S, Na S, and Rathnachalam R (2005) Noncalcemic actions of vitamin D receptor ligands. *Endocr Rev* **26:**662–687.
Nakabayashi M, Yamada S, Yoshimoto N, Tanaka T, Igarashi M, Ikura T, Ito N, Makishima M, Tokiwa H, DeLuca HF, et al. (2008) Crystal structures of rat vitamin D receptor bound to adamantyl vitamin D analogs: structural basis for vitamin D receptor antagonism and partial agonism. *J Med Chem* **51:**5320–5329.
Nishida S, Ozeki J, and Makishima M (2009) Modulation of bile acid metabolism by 1α-hydroxyvitamin D_3 administration in mice. *Drug Metab Dispos* **37:**2037–2044.
Pathrose P, Barmina O, Chang CY, McDonnell DP, Shevde NK, and Pike JW (2002) Inhibition of 1,25-dihydroxyvitamin D_3-dependent transcription by synthetic LXXLL peptide antagonists that target the activation domains of the vitamin D and retinoid X receptors. *J Bone Miner Res* **17:**2196–2205.
Peräkylä M, Malinen M, Herzig KH, and Carlberg C (2005) Gene regulatory potential of nonsteroidal vitamin D receptor ligands. *Mol Endocrinol* **19:**2060–2073.
Prüfer K, Racz A, Lin GC, and Barsony J (2000) Dimerization with retinoid X receptors promotes nuclear localization and subnuclear targeting of vitamin D receptors. *J Biol Chem* **275:**41114–41123.
Rosenfeld MG, Lunyak VV, and Glass CK (2006) Sensors and signals: a coactivator/corepressor/epigenetic code for integrating signal-dependent programs of transcriptional response. *Genes Dev* **20:**1405–1428.
Sánchez-Martínez R, Zambrano A, Castillo AI, and Aranda A (2008) Vitamin D-dependent recruitment of corepressors to vitamin D/retinoid X receptor heterodimers. *Mol Cell Biol* **28:**3817–3829.
Schaufele F, Carbonell X, Guerbadot M, Borngraeber S, Chapman MS, Ma AA, Miner JN, and Diamond MI (2005) The structural basis of androgen receptor activation: Intramolecular and intermolecular amino-carboxy interactions. *Proc Natl Acad Sci USA* **102:**9802–9807.
Shang Y, Hu X, DiRenzo J, Lazar MA, and Brown M (2000) Cofactor dynamics and sufficiency in estrogen receptor-regulated transcription. *Cell* **103:**843–852.
Tagami T, Lutz WH, Kumar R, and Jameson JL (1998) The interaction of the vitamin D receptor with nuclear receptor corepressors and coactivators. *Biochem Biophys Res Commun* **253:**358–363.
Väisänen S, Dunlop TW, Sinkkonen L, Frank C, and Carlberg C (2005) Spatio-temporal activation of chromatin on the human CYP24 gene promoter in the presence of 1α,25-dihydroxyvitamin D_3. *J Mol Biol* **350:**65–77.
Zwart W, Griekspoor A, Berno V, Lakeman K, Jalink K, Mancini M, Neefjes J, and Michalides R (2007) PKA-induced resistance to tamoxifen is associated with an altered orientation of ERα towards co-activator SRC-1. *EMBO J* **26:**3534–3544.

Address correspondence to: Makoto Makishima, Division of Biochemistry, Department of Biomedical Sciences, Nihon University School of Medicine, Itabashi-ku, Tokyo 173-8610, Japan. E-mail: makishima.makoto@nihon-u.ac.jp